crystals

MDPI

Review

Manipulation of Crystallization Kinetics for Perovskite Photovoltaics Prepared Using Two-Step Method

Fei Wang [1,2], Chuangye Ge [2], Xianfang Zhou [1,2], Xiao Liang [1,2], Dawei Duan [2], Haoran Lin [2], Quanyao Zhu [1,*] and Hanlin Hu [2,*]

1   State Key Laboratory of Advanced Technology for Materials Synthesis and Processing, School of Materials Science and Engineering, Wuhan University of Technology, Wuhan 430070, China; feiwang@whut.edu.cn (F.W.); 257508@whut.edu.cn (X.Z.); liangxiao1414@whut.edu.cn (X.L.)
2   Hoffman Institute of Advanced Materials, Shenzhen Polytechnic, 7098 Liuxian Boulevard, Shenzhen 518055, China; gcy_xfz@szpt.edu.cn (C.G.); duandwthu@szpt.edu.cn (D.D.); hlin@szpt.edu.cn (H.L.)
*   Correspondence: cglamri@whut.edu.cn (Q.Z.); hanlinhu@szpt.edu.cn (H.H.)

Abstract: Two-step fabricated perovskite solar cells have attracted considerable attention because of their good reproducibility and controllable crystallization during production. Optimizing the quality of perovskite films plays a decisive role in realizing superb performance via a two-step method. Many breakthroughs have been achieved to obtain high-quality film from the perspective of manipulating crystallization kinetics in the two-step preparation process, which promotes the rapid development of perovskite photovoltaics. Therefore, focusing on the crystallization process in the two-step preparation process can provide a reliable basis for optimizing the performance of two-step devices. In this review, recent progress on regulating the crystallization process for two-step PSCs is systematically reviewed. Firstly, a specific description and discussion are provided on the crystallization process of perovskite in different two-step methods, including spin-coating, immersion and evaporation. Next, to obtain high-quality perovskite film via these two-step methods, current strategies of additive engineering, composition engineering, and solvent engineering for regulating the crystallization process for two-step perovskite are classified and investigated. Lastly, the challenges which hindering the performance of the two-step perovskite photovoltaics and an outlook toward further developments are proposed.

Keywords: two-step; perovskite crystallization; kinetics; solar cells

1. Introduction

Perovskite solar cells (PSCs) have been regarded as the star materials of the next generation in the photovoltaic field due to their superior efficiency (over 25.8%) [1,2]. Abundant studies have concentrated on the quality of perovskite films, which plays a decisive role in improving the efficiency of perovskite devices [3]. At present, methods of preparing high-quality perovskite films with a free pinhole mainly include one-step and two-step methods [4].

In 2009, a precursor solution of CH_3NH_3I and PbI_2 in γ-butyrolactone was employed to prepare an $MAPbI_3$ film by Kojima and colleagues through a one-step spin-coating methods, and the first $MAPbI_3$-based PSC displayed a power conversion efficiency (PCE) of 3.8% [5]. Although this achievement provided a groundbreaking foundation for the subsequent development of perovskite devices, the poor quality of perovskite films prepared using the one-step method directly affects their efficiency. To address this issue, Seok et al. [6]. proposed an anti-solvent-assisted one-step strategy to acquire a uniform perovskite film by introducing toluene as an anti-solvent. However, most high-efficiency PSCs prepared using the anti-solvent-assisted one-step method employ toxic anti-solvents, such as chlorobenzene (CB), toluene, and dichloromethane (DCM), which impedes the commercialization of

PSCs [7,8]. In addition, the application of anti-solvent is plagued by operational challenges in the preparation process of high-performance devices.

By contrast, the two-step method is generally considered to possess better repeatability and controllability of the crystallization process [9–13]. Grätzel and coworkers first developed a two-step method for the fabrication of PSCs with a PCE of 15% [14]. The fabrication of perovskite film using the two-step method involved two processes: the introduction of lead iodide (PbI_2) onto the nanostructured titanium dioxide (TiO_2) film through the spin-coating process and subsequent immersion into CH_3NH_3I solution. In 2014, Park and colleagues applied a two-step spin-coating procedure for PSCs to achieve a PCE of 17.01% [15]. Aiming at expanding the active area of devices, evaporation technology was also introduced into the two-step method, combined with spin-coating to promote the fabrication of large-area devices. In order to further optimize the quality of perovskite films for obtaining high-efficiency PCSs through these two-step methods, more attention has been focused on understanding and controlling the crystallization process of the perovskite film from the aspects of additive, composition, solution, and interfacial modification engineering. You and colleagues found that the incorporation of 5% (volume ratio) dimethyl sulfoxide (DMSO) in N,N-dimethylformamide (DMF) could slow the crystallization of PbI_2 due to the formation of a PbI_2–DMSO complex, leading to a dense and smooth PbI_2 layer [16]. The corresponding device realized a PCE of 21.6% for a small size (active area of 0.0737 cm^2) and 20.1% for a large size (active area of 1 cm^2). In 2020, Lu et al. [17] employed composition engineering of sequential A-site doping using a two-step method to control the perovskite crystallization kinetics, showing an enhanced PCE up to 23.5%. Recently, Sun and coworkers utilized biguanide hydrochloride (BGCl) as an interfacial modifier at the interface of tin oxide (SnO_2)/perovskite to anchor the I/I^- in PbI_2 via hydrogen bonding, endowing the homogeneous crystal growth of the PbI_2 and perovskite film and PSCs with a PCE of 24.4% [18]. This research progress on optimization of the crystallization for highly efficient PSCs using a two-step method demonstrates the potential of two-step PSCs, promoting their further commercialization.

In this review, we provide a comprehensive understanding toward manipulating the crystallization kinetics of perovskite via a two-step method for efficient and stable PSCs. In particular, we first conduct a systematic analysis of and discussion on the crystallization process of perovskite via various two-step methods, such as spin-coating, immersion, and evaporation. Then, we provide an overview of recent progress in the crystallization strategies of additive engineering, composition engineering, and solution engineering using two-step methods for PSCs. Lastly, we propose the challenges facing the manipulation of crystallization kinetics, as well as an outlook toward the future development of the two-step method for PSCs.

2. Crystallization Process of Perovskite Using Two-Step Method

A variety of two-step preparation processes have been developed to fabricate high-quality perovskite films and corresponding devices. According to the distinction of technology, the two-step preparation processes can be mainly divided into immersion, spin-coating, and evaporation methods, as shown in Figure 1. The specific preparation processes of different methods and the related factors affecting perovskite crystallization are discussed in this section.
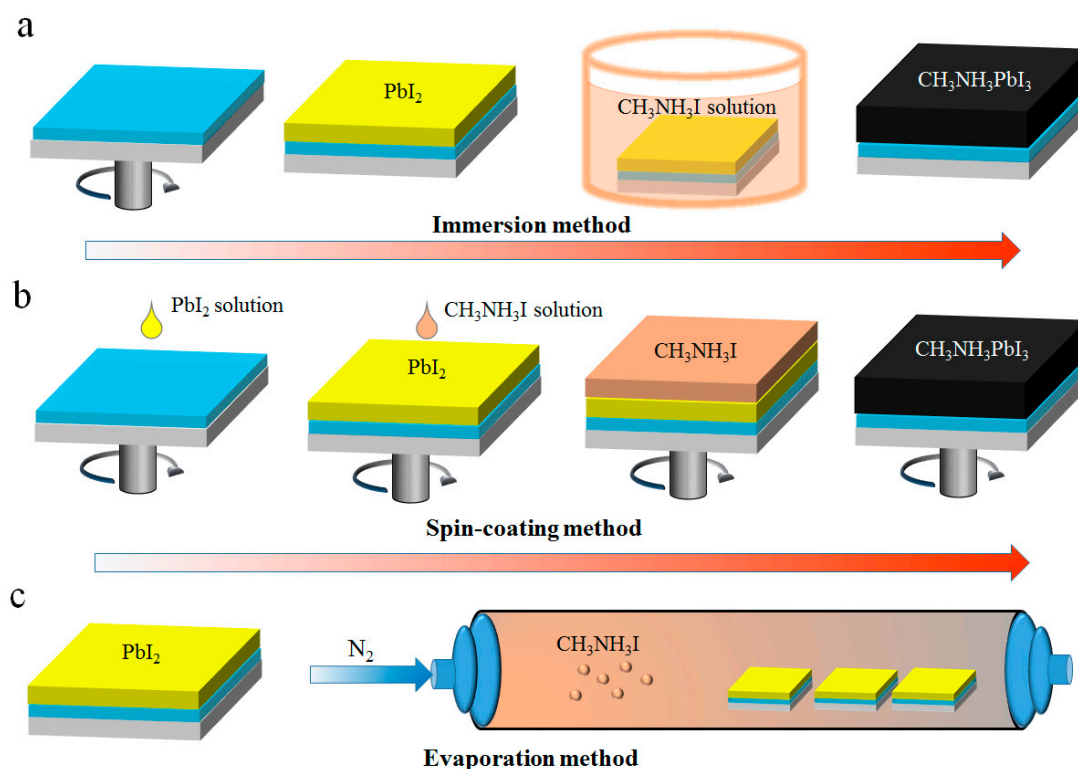
Figure 1. Schematic diagram of different types of two-step methods: (**a**) immersion, (**b**) spin-coating, and (**c**) evaporation two-steps methods for the fabrication of perovskite film.

2.1. Immersion Method

The immersion method as the primary process for two-step perovskite devices was created by Grätzel and colleagues in 2013 [14]. PbI_2 was first introduced on top of titanium dioxide through spin-coating technology; the formed PbI_2 film was subsequently exposed to a CH_3NH_3I solution to complete the crystallization process of perovskite, as shown in Figure 1a. Both steps have a significant effect on the morphology and crystallization process of perovskite films in this immersion method. The different thickness and morphology of PbI_2 films obtained by spin coating with different parameters directly affect the subsequent crystallization process of perovskite in the immersion process. Using the immersion method, the PSCs fabricated by sequential deposition displayed the best PCE of 15% with high reproducibility, providing a research basis for subsequent two-step perovskite devices based on the immersion method.

An in-depth understanding and efficient optimization of the crystallization process during the two-step method is regarded as a key point in obtaining high-quality perovskite films. Jin and coworkers systematically investigated the crystal growth process of the perovskite materials and proposed two different growth mechanisms (a solid–liquid interfacial conversion reaction and a dissolution recrystallization growth mechanism) of crystalline $CH_3NH_3PbI_3$ nanostructures based on different concentrations of CH_3NH_3I [19]. At a low concentration (≤ 8 mg/mL) of CH_3NH_3I, CH_3NH_3I diffused into layered PbI_2 to undergo the solid–liquid interfacial conversion reaction for the formation of $CH_3NH_3PbI_3$, while the further diffusion of CH_3NH_3I was inhibited by the formed crystalline $CH_3NH_3PbI_3$ on the surface, leading to suppression of this interfacial conversion reaction. When the concentration of CH_3NH_3I solution was higher than 10 mg/mL, a perovskite layer formed rapidly on the surface, which seriously affected the diffusion of CH_3NH_3I and hindered the conversion to perovskite. However, when the CH_3NH_3I solution concentration was further increased to ≥ 20 mg/mL, the high concentration of I^- promoted the formation of lead iodide complex ions (PbI_4^{2-}), which contributed to the dissolution of formed $CH_3NH_3PbI_3$ and unconverted PbI_2 until it reached saturation. The PbI_4^{2-} subsequently reacted with

$CH_3NH_3^+$ to form $CH_3NH_3PbI_3$ crystals via a slow crystallization process. In order to further realize the influence factor of perovskite crystallization in the immersion method, Liu and coworkers investigated the effect of PbI_2 morphology on the subsequent crystallization of the perovskite film by controlling the growth time of PbI_2 and $CH_3NH_3PbI_3$; they employed the UV–Vis absorption spectra to detect the growth of PbI_2 grains [20]. According to the enhanced light absorption with the time increasing from 0 to 7 min, the continuous crystal growth phenomenon of PbI_2 was speculated during this period. From 7 to 9 min, the almost constant absorption indicated that the grain size of PbI_2 reached saturation. The crystallization of perovskite was also determined by the immersion time [21,22] and post-treatment process [23,24].

2.2. Spin-Coating Method

Among the two-step methods for the fabrication of efficient and stable PSCs, the two-step spin-coating method is the most commonly used [25–27]. Generally, in the two-step spin-coating method, PbI_2 and CH_3NH_3I are first dissolved in DMF and isopropanol (IPA) solutions [28], respectively. The PbI_2 solution is spin-coated on the ETL to form a dense PbI_2 film after thermal annealing. The organic component CH_3NH_3I solution was deposited on the dense PbI_2 film and sintered on the substrate as shown in Figure 1b. A perovskite thin film was formed through the internal diffusion of CH_3NH_3I and PbI_2 during this two-step spin-coating process. With I^- in CH_3NH_3I as the electron donor, the reaction of inorganic PbI_2 with organic CH_3NH_3I is generally considered as pseudo-intercalation, and PbI_2 first reacts with I^- to form $(PbI_3)^-$ through the I_2–I^- interaction, before undergoing a reaction with $CH_3NH_3^+$ to form $CH_3NH_3PbI_3$ [29]. The internal diffusion and morphology of perovskite thin films were affected by the speed of spin-coating the PbI_2 solution and FAI solution in the two-step process. You and colleagues applied a fixed speed of 1500 rpm for PbI_2 and different speeds for FAI (1000, 1300, 1500, and 1700 rpm), which exerted a specific influence on the obtained perovskite film [16]. The residue of PbI_2 gradually increased with the increase in rotating speed, indicating that the change in rotating speed can determine the transformation from lead iodide to perovskite.

Huang and colleagues systematically investigated the distinction of the internal diffusion of CH_3NH_3I and PbI_2 and the crystallization of perovskite using the spin-coating and the immersion two-step method [30]. The arduous diffusion of CH_3NH_3I into the thick PbI_2 and the rapid crystallization process of perovskite during the immersion method led to a rough and unsatisfactory morphology, resulting in a low performance of 3.2%. The contrast with thermal annealing in the two-step spin-coating method is obvious, which can promote the permeation of CH_3NH_3I into PbI_2 to form a dense perovskite film. The growth mechanism of $CH_3NH_3PbI_3$ cuboids in the two-step spin-coating process was thoroughly researched by Park and coworkers [15]. In the growth process of $CH_3NH_3PbI_3$, the CH_3NH_3I concentration was regarded as the critical factor determining the size and shape of the formed $CH_3NH_3PbI_3$ cuboids, and the size of the $MAPbI_3$ cuboids was negatively correlated with CH_3NH_3I concentration. In a system with low CH_3NH_3I concentration, the formation of bigger cuboid sizes was observed due to the separate distribution of seed crystals, whereas the suppression of further crystal growth was discovered in a system with higher concentration because of the terminated nucleation and growth at the primary stage. In addition to the factor of CH_3NH_3I concentration, other factors such as reacting temperature [31,32] and post-treatments [26] have been proven to affect the crystallization process of perovskite in the two-step method. Cho and colleagues divided the crystallization process into two processes according to the distinct kinetics and analyzed the effect of different reaction temperatures on the nucleation and growth processes of perovskite [32]. The reaction of PbI_2 and CH_3NH_3I to form perovskite crystals occurred on the surface in the first process, and this reaction involved both the nucleation and the growth of perovskite crystals. During the second process, CH_3NH_3I molecules reacted with the buried PbI_2 through the diffusion of CH_3NH_3I across the intergrain gaps in the surface perovskite layer under the sufficient thermal energy provided by heating. In order to gain an in-depth un-

derstanding of the crystallization process of perovskite in the two-step method, Panzer et al. employed in situ absorption and photoluminescence spectroscopy to trace the formation of a two-step MAPbI$_3$ thin film via interface crystallization and dissolution–recrystallization processes during the spin-coating process [33].

2.3. Evaporation Technology

Unlike the spin-coating and immersion methods, evaporation technology is applied for the fabrication of dense perovskite, especially in large-area films, highlighting the potential of evaporation technology for the commercialization of PSCs [34,35]. PbI$_2$ was first deposited on the transport layer by spin-coating or evaporation method, before forming PbI$_2$ thin films through thermal annealing as shown in Figure 1c. Then, an organic salt solution was deposited on the PbI$_2$ thin films via the evaporation method. Currently, two-step methods based on evaporation technology can be mainly divided into the full evaporation method [36] and the hybrid solvent–vapor method [37,38]. In 2014, Lin and colleagues proposed a full evaporation method to fabricate a uniform CH$_3$NH$_3$PbI$_{3-x}$Cl$_x$ film [39]. Dense lead(II) chloride (PbCl$_2$) films were firstly deposited onto the poly(3,4-ethylenedioxythiophene)/poly(styrenesulfonate) (PEDOT:PSS)-coated indium tin oxide (ITO) glass through thermal evaporation in a high-vacuum chamber, and CH$_3$NH$_3$I was then sublimed onto PbCl$_2$ films to form the perovskite thin film. In this simple sequential vacuum deposition, the reaction extent between PbCl$_2$ and CH$_3$NH$_3$I and the morphologies of perovskite film were optimized by the substrate temperature, resulting in a uniform perovskite film with large-scale homogeneous crystalline structures. To improve the reproducibility of the traditional full evaporation method, Qi et al. [40] employed a hybrid physical–chemical deposition method (HCVD) using multizone equipment with independent and controlled pressure, temperature, and gas flow rate for manufacturing the perovskite film. This process mainly involved two evaporation steps: (1) PbCl$_2$ was first deposited onto the substrates via thermal evaporation under a high vacuum and placed into the furnace in the low-temperature zone; (2) the MAI was heated to an appropriate temperature in another region in the high-temperature zone of the furnace to form the vapor phase and reacted with the PbCl$_2$. Various factors, such as PbCl$_2$ layer thickness, MAI deposition temperature, annealing temperature, and annealing time, were considered to have an effect on the crystallization process of perovskite and, thus, affect the quality of perovskite films in this two-step HCVD method [41,42].

In contrast to the harsh vacuum environment requirements in the full evaporation method, the solvent–vapor hybrid method is not limited to a vacuum environment, whereby PbI$_2$ is coated onto the transport layer through traditional solution processing methods and CH$_3$NH$_3$I power is subsequently evaporated to form the perovskite film. Chen and colleagues reported a low-pressure hybrid evaporation method for the fabrication of CH$_3$NH$_3$PbI$_3$ perovskite films; specifically, PbI$_2$ film prepared using the spin-coating method in advance was placed into the low-pressure heating tube setup to react with the thermal evaporated CH$_3$NH$_3$I composition, thus forming the perovskite film [43]. In order to obtain high-quality films, the effects of pressure and reaction periods in the chemical vapor deposition step on perovskite crystallization were discussed. Extremely low MAI vapor partial pressure is favorable for the formation of uniform perovskite crystals, whereas exaggerated pressure induces the incomplete reaction between vaporized MAI and PbI$_2$. The reaction time of MAI and PbI$_2$ also affected the crystallization of perovskite according to an analysis of the reaction mechanism of gas–solid crystallization kinetics and thermodynamics. The short reaction time induced the incomplete conversion of PbI$_2$ into perovskite, whereas the prolonged reaction time caused the partial decomposition of CH$_3$NH$_3$PbI$_3$ into PbI$_2$ and MAI.

3. Strategies for Manipulating Crystallization Kinetics

The composition, solvents, and additives in the perovskite precursor solution affect the crystallization processes of perovskite, leading to some differences in the morphology

and uniformity of the perovskite film, as well as the photovoltaic properties of device [44]. Therefore, controlling the crystallization process of perovskite through different strategies, including additive engineering, composition engineering, and solvent engineering, plays a decisive role in obtaining high-quality films, with corresponding efficient and stable PSCs, as shown in Figure 2 and Table 1. Abundant research attention has been directed toward the selection and optimization of solution, composition, and additives through these strategies, so as to understand their specific impact on the crystallization process of perovskite.

3.1. Additive Engineering

Some studies on additive engineering for the crystallization control of perovskite in the two-step process are summarized in Table 1. In additive engineering, various kinds of additives such as salts [45,46], polymers [47], low-dimensional perovskite [48], and ionic liquids (ILs) [49,50] have been introduced to control the crystallization process of perovskite. In two-step PSCs, these additives are normally incorporated into inorganic or organic components for optimizing the crystallization process. Qi and colleagues applied ammonium chloride (NH_4Cl) as an additive in the inorganic PbI_2 precursor solution to regulate the crystallization process of two-step perovskite [46]. The NH_4^+ cations in NH_4Cl diffused into the PbI_2 layer, leading to the formation of intermediate unstable phases of $x[NH_4^+]\cdot[PbI_2Cl_x]^{x-}$, which transformed immediately into other intermediate phases of $HPbI_{3-x}Cl_x$. Thus, the formation and existence of the intermediate phases effectively retarded the crystallization of perovskite, resulting in a uniform film with high crystallinity and large grain sizes. Taking advantage of NH_4Cl additive engineering, the NH_4Cl-treated PSCs based on the high-quality perovskite film achieved a PCE of 20.17% with the designated area of 0.09 cm^2 and a PCE of 14.55% with the designated area of 22.4 cm^2. Other salt additives such as n-butylammonium bromide (BABr) [51] and nickel chloride ($NiCl_2$) [52] have been employed in the inorganic PbI_2 precursor solution to manipulate the crystallization process in two-step PSCs. Our group employed 1D trimethyl sulfonium lead triiodide (Me_3SPbI_3) in 3D perovskite to form a 1D/3D composite perovskite layer with improved crystallinity and morphology [48]. The relevant 1D/3D PSCs achieved the best PCE of 22.06% and maintained 97% of the original efficiency after 1000 h of storage in conditions of relative humidity (RH) = 50% without encapsulation. Trimesic acid (TMA) was introduced into the PbI_2 precursor solution by Zhu and coworkers to form the intermediate phase through the coordination among three carboxyl groups in TMA and Pb^{2+}, lengthening the crystallization process of perovskite film [53]. The acid additive engineering caused a delayed crystallization of perovskite, and this was regarded as an effective approach to fabricate a high-quality film with increased crystallinity and uniformity [54].

In contrast to these traditional additives, ILs have been considered as green additives to assist in the crystallization process of perovskite due to their nonvolatile characteristics. Zhang and colleagues reported an additive engineering approach via an immersion-based two-step method through the introduction of IL 1-butyl-3-methylimidazolium iodide (BMII) into the PbI_2 precursor solution [57]. The coordination interaction between BMII and PbI_2 led to a ligand-exchange process, which hindered the reaction of MAI with PbI_2, thus delaying the crystallization process of perovskite. The introduction of IL BMII endowed the perovskite film with increased crystallinity and fewer defects.

Furthermore, additives were also employed in the organic precursor solution to regulate the crystallization. Zhou and colleagues employed a series of alkaline materials such as formamidine acetate (FAAc), sodium acetate (CH_3COONa), sodium hydroxide (NaOH), and potassium hydroxide (KOH) as additives to deeply investigate the effect of alkaline additives on the crystallization kinetics of perovskite [58]. In the CH_3COONa and FAAc system, the acetate ions promoted grain growth, thus resulting in a uniform perovskite film with a larger grain size (~1μm) than the reference film (~300 nm), whereas a similar grain size and distinct crystalline grains were obtained in the system of NaOH or KOH compared with the reference film. Wang et al. [59]. proposed an additive engineering approach

via adding trimethylammonium chloride (TACl) to the MAI precursor solution to obtain perovskite films with decreased grain boundaries and trap densities. The corresponding TACl-treated PSCs realized the best PCE of 20.92% and a high V_{OC} of 1.15 V.
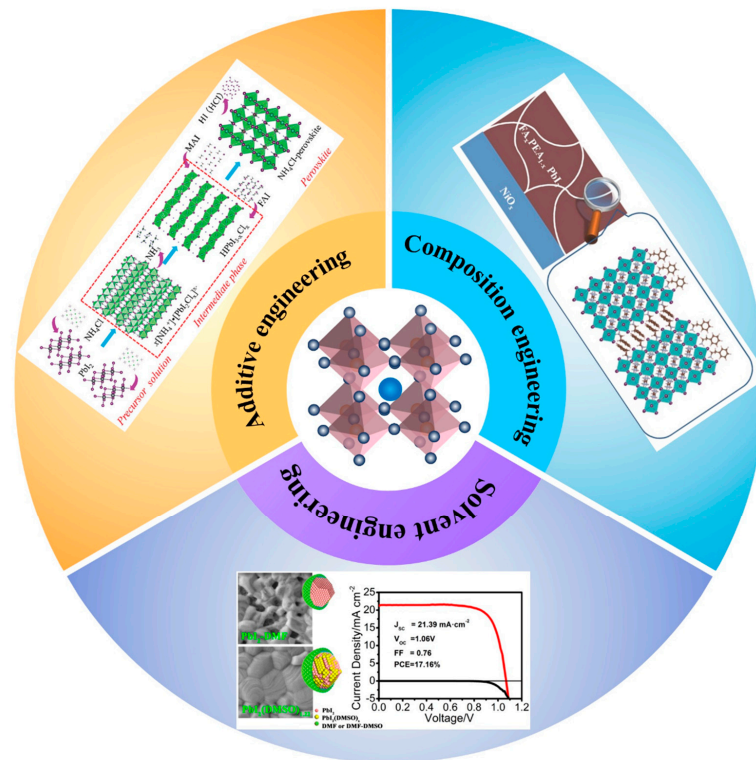

Figure 2. Different strategies for manipulating crystallization kinetics in two-step PSCs. Additive engineering image: reprinted with permission from [46]; copyright 2021, the authors; published by Wiley-VCH. Composition engineering image: reprinted with permission from [55]; Copyright 2016; Wiley-VCH. Solvent engineering image: reprinted with permission from [56]; Copyright 2015; American Chemical Society.

Table 1. Summary of some strategies for manipulating crystallization kinetics using a two-step process.

Strategies	Perovskite Component	Jsc (mA/cm^2)	V_{OC} (V)	FF (%)	PCE (%)	Ref.
Additive engineering	$Cs_{0.05}FA_{0.54}MA_{0.41}Pb(I_{0.98}Br_{0.02})_3$	23.01	1.110	78.97	20.17	[46]
Additive engineering	$(FAPbI_3)_{1-x}(MAPbBr_3)_x$	24.40	1.180	79.00	22.70	[51]
Additive engineering	$MAPbI_3$	22.64	1.130	81.00	20.61	[52]
Additive engineering	1D/3D perovskite	24.64	1.140	78.57	22.07	[48]
Additive engineering	$MAPbI_3$	23.54	1.030	71.00	17.21	[53]
Additive engineering	$MAPbI_3$	18.60	0.894	62.00	10.20	[54]
Additive engineering	$MAPbI_3$	21.58	1.040	70.00	15.60	[57]
Additive engineering	$(FA, MA, Cs)Pb(I, Br)_3$	24.05	1.145	76.31	21.01	[58]
Additive engineering	$MAPbI_3$	22.57	1.150	80.58	20.92	[59]
Composition engineering	$FA_xPEA_{1-x}PbI_3$	22.08	1.040	77.13	17.71	[55]
Composition engineering	$MAPbI_3$	23.05	1.060	65.35	15.64	[60]
Composition engineering	$Cs_x(MA_{0.4}FA_{0.6})_{1-x}PbI_3$	23.30	1.081	80.80	20.30	[61]
Composition engineering	$CH_3NH_3PbI_{3-x}(SCN)_x$	21.10	0.956	75.00	15.12	[62]
Composition engineering	$FAPbI_3$	25.00	1.110	81.70	22.60	[63]
Composition engineering	$(GA_{1/16}Cs_{1/16}FA_{14/16})Pb(I_{15/16}Br_{1/16})_3$	24.80	1.160	81.30	23.50	[17]
Solvent engineering	$MAPbI_3$	20.71	1.020	64.00	13.50	[64]
Solvent engineering	$MAPbI_3$	21.39	1.060	76.00	17.16	[56]
Solvent engineering	$MAPbI_3$	22.55	1.010	71.00	16.17	[65]
Solvent engineering	$FASnI_3$	17.37	0.530	73.47	6.80	[66]
Solvent engineering	$FASnI_3$	19.96	0.770	65.70	10.09	[67]

3.2. Composition Engineering

PbI_2 and MAI (FAI) were employed as the primary inorganic and organic components to fabricate an $MAPbI_3$ ($FAPbI_3$) film via the two-step method [68]. However, this perovskite film exhibited unsatisfactory crystallinity, uniformity, and stability, hindering the further development of corresponding devices [69]. In order to enhance the quality of the perovskite film, other types of inorganic and organic compositions of lead(II) thiocyanate ($Pb(SCN)_2$) [62], lead(II) acetate ($PbAc_2$) [60], phenylethylammonium iodide (PEAI) [55], and cesium iodide (CsI) [17,61] have been adopted to tune the crystallization process of perovskite through composition engineering. These composition engineering approaches are also summarized in Table 1. Meng and coworkers thoroughly investigated the application of CsI for controlling the crystallization of perovskite [61]. After the incorporation of CsI into the PbI_2 solution, the formative intermediate phase through the coordination among Pb^{2+}, DMSO, and Cs^+ efficiently delayed the crystallization of PbI_2 film and inhibited the formation of the yellow non-perovskite δ-phase, resulting in a uniform perovskite film with larger grains and fewer defects.

Lu and colleagues traced the effect of sequential A-site doping of Cs^+ and guanidinium (GA^+) on the crystallization process of $FAPbI_3$-based perovskites through in situ grazing incidence wide-angle X-ray scattering (GIWAXS) measurements [17]. Specially, CsI and GAI were added to the PbI_2 solution and organic salt solution to precisely control the perovskite crystallization kinetics and form a high-quality film. In the deposition process of PbI_2, the incorporation of Cs exhibited the distinct crystallization pathway compared to PbI_2 without Cs^+, leading to the formation of dominant δ-$CsPbI_3$ and the suppression of PbI_2 phases. In the subsequent organic layer deposition process, the introduction of GA^+ led to a relatively accelerated phase conversion from δ-$CsPbI_3$ to the perovskite phase, which was attributed to the faster crystal growth of perovskites. With the optimization of doping concentrations of Cs^+ and GA^+, the as-prepared perovskite films exhibited a higher crystallinity and reduced defect density, and the relevant PSCs achieved the best PCE of 23.5%. Seok and his colleagues adjusted the composition of $FAPbI_3$ by incorporating a handful of $MAPbBr_3$ to undergo a modified intramolecular exchange process [63]. By means of this composition engineering approach, the crystalline a-$FAPbI_3$ phase was markedly increased and the concentration of defects was reduced, leading to a certified PCE of 22.1%. Unlike doping with small cations (MA^+, FA^+, or Cs^+), phenylethylammonium iodide (PEAI) was also incorporated by Jen et al. into the $FAPbI_3$ perovskite lattice to obtain the mixed cation $FA_xPEA_{1-x}PbI_3$ using the two-step method [55], obtaining perovskite films with a smooth and homogenous morphology.

3.3. Solvent Engineering

In the initial two-step preparation process, DMF is generally employed as the solvent in the step of PbI_2 deposition. However, the fast crystallization of PbI_2 in DMF generates PbI_2 crystals with different sizes and causes the incomplete conversion of PbI_2, leading to an uncontrolled morphology of the perovskite film. The studies based on solvent engineering for the crystallization control of perovskite via a two-step process are summarized in Table 1. Han and colleagues proposed a solvent strategy employing DMSO as a solvent to replace DMF for the preparation of PbI_2 films [64]. DMSO possessed a stronger coordination ability with PbI_2 than DMF, which retarded the crystallization of PbI_2, resulting in a uniform PbI_2 film. The uniform PbI_2 provided the basis for the formation of a high-quality perovskite film with homogeneous grain sizes. More importantly, the formed perovskite film and related devices exhibited better repeatability. In order to further control the crystallization process of perovskite in the two-step method, Wang and coworkers systematically researched the effect of different ratios between DMSO and DMF on the crystallization process, film morphology, and device performance [56]. The presence of a coordination interaction between PbI_2 and DMSO induced the generation of the $PbI_2(DMSO)_x$ complex in the DMF/DMSO solvent system, and the formed $PbI_2(DMSO)_x$ complexes exhibited a homogeneous distribution in the DMF. With an increase in the

ratio of DMSO in the mixed solvent, the intensity of the peak ascribed to perovskite was strengthened, suggesting that DMSO or $PbI_2(DMSO)_x$ promoted the crystal growth of the perovskite film. As a result, the DMF/DMSO solvent engineering endowed the PSCs with a PCE of 17.16%, a V_{OC} of 1.06 V, a J_{SC} of 21.39 mA/cm^2, and an FF of 0.76.

In addition to the common solvent DMSO, N-pyrrolidone (NMP) and hexamethylphosphoric triamide (HMPA) were explored as co-solvents in DMF systems to fabricate perovskite films by Wei and colleagues [65]. The incorporation of these solvents led to pores in the PbI_2 film due to the formative intermediate phase $PbI_2 \cdot x$Sol, which accelerated the conversion from PbI_2 to perovskite. Moreover, solvent engineering also plays a significant role in manipulating the crystallization kinetics of Sn-based perovskite [66]. The rapid crystallization process of Sn-based perovskite was regarded as the dominant cause of perovskites with poor-quality films, hindering the further development of Sn-based PSCs [70]. Han and coworkers [67] investigated the steric hindrance of four kinds of solvents, isopropyl alcohol (IPA), 2-methyl-1-propanol, 3-methyl-1-butanol, and 2-methyl-2-butanol, in the Sn-based perovskite crystallization process. The results indicated that the presence of the strongest steric hindrance with hydroxyl in the 2-methyl-2-butanol contributed significantly to obtaining high-quality perovskite films with a dense and uniform morphology, generating a PCE increase to 10.09%.

4. Outlook and Challenges

In this review, we provided a comprehensive understanding of the recent progress and breakthroughs in manipulating the crystallization kinetics for two-step perovskite photovoltaics. In particular, the overall description and discussion were concentrated on the crystallization process of perovskite and the strategies for manipulating crystallization kinetics via a two-step method. We introduced and summarized the specific processes and the factors affecting the crystallization process of various two-step methods, including spin-coating, immersion, and evaporation. Considering the optimization of the crystallization process in these two-step processes, the strategies for manipulating crystallization kinetics from the aspects of additive engineering, composition engineering, and solvent engineering were targeted to obtain high-quality two-step perovskite films and high-performance devices. In additive engineering, the specific impacts of different types of additives in the precursor solutions on the crystallization process of perovskite were investigated. In composition or solvent engineering, researchers concentrated on the substitution or optimization of traditional components or solvents to improve the crystallization process of perovskite. Even though remarkable progress in manipulating the crystallization kinetics of two-step PSCs has been achieved, there are still many challenges to be solved to further promote the development of PSCs. Hence, we summarize the current challenges and prospects as follows:

(1) The mechanism of manipulating crystallization kinetics needs an in-depth study. It is necessary to employ in situ technology (in situ X-ray diffraction (XRD), grazing-incidence wide-angle X-ray scattering (GIWAXS), photoluminescence (PL), and UV–Vis absorption) to track the crystallization process in real time from the aspects of crystallization rate, phase purity, orientation, etc.

(2) Starting from the structure, as well as chemical and physical properties of the materials, novel materials possessing the advantages of simple preparation, low toxicity, and high stability must be developed for manipulating the crystallization kinetics of two-step perovskite photovoltaics.

(3) These strategies for manipulating the crystallization kinetics can be further extended to large-area or flexible devices toward various technologies (spin-coating, blade-coating, slot-die coating, blade coating, inkjet printing, and spray-coating) based on two-step preparation, to explore their practical applications in the future.

References

1. Jeong, J.; Kim, M.; Seo, J.; Lu, H.; Ahlawat, P.; Mishra, A.; Yang, Y.; Hope, M.A.; Eickemeyer, F.T.; Kim, M.; et al. Pseudo-Halide Anion Engineering for α-FAPbI$_3$ Perovskite Solar Cells. *Nature* **2021**, *592*, 381–385. [CrossRef]

2. Min, H.; Lee, D.Y.; Kim, J.; Kim, G.; Lee, K.S.; Kim, J.; Paik, M.J.; Kim, Y.K.; Kim, K.S.; Kim, M.G.; et al. Perovskite Solar Cells with Atomically Coherent Interlayers on SnO$_2$ Electrodes. *Nature* **2021**, *598*, 444–450. [CrossRef] [PubMed]

3. Yang, W.S.; Noh, J.H.; Jeon, N.J.; Kim, Y.C.; Ryu, S.; Seo, J.; Seok, S. Il High-Performance Photovoltaic Perovskite Layers Fabricated through Intramolecular Exchange. *Science* **2015**, *348*, 1234–1237. [CrossRef]

4. Zheng, X.; Chen, B.; Dai, J.; Fang, Y.; Bai, Y.; Lin, Y.; Wei, H.; Zeng, X.C.; Huang, J. Defect Passivation in Hybrid Perovskite Solar Cells Using Quaternary Ammonium Halide Anions and Cations. *Nat. Energy* **2017**, *2*, 17102. [CrossRef]

5. Kojima, A.; Teshima, K.; Shirai, Y.; Miyasaka, T. Organometal Halide Perovskites as Visible-Light Sensitizers for Photovoltaic Cells. *J. Am. Chem. Soc.* **2009**, *131*, 6050–6051. [CrossRef]

6. Jeon, N.J.; Noh, J.H.; Kim, Y.C.; Yang, W.S.; Ryu, S.; Seok, S. Il Solvent Engineering for High-Performance Inorganic–organic Hybrid Perovskite Solar Cells. *Nat. Mater.* **2014**, *13*, 897–903. [CrossRef] [PubMed]

7. Zhang, M.; Wang, Z.; Zhou, B.; Jia, X.; Ma, Q.; Yuan, N.; Zheng, X.; Ding, J.; Zhang, W.H. Green Anti-Solvent Processed Planar Perovskite Solar Cells with Efficiency beyond 19%. *Sol. RRL* **2018**, *2*, 1700213. [CrossRef]

8. Shan, S.; Li, Y.; Wu, H.; Chen, T.; Niu, B.; Zhang, Y.; Wang, D.; Kan, C.; Yu, X.; Zuo, L.; et al. Manipulating the Film Morphology Evolution toward Green Solvent-processed Perovskite Solar Cells. *SusMat* **2021**, *1*, 537–544. [CrossRef]

9. Bi, D.; Moon, S.J.; Häggman, L.; Boschloo, G.; Yang, L.; Johansson, E.M.J.; Nazeeruddin, M.K.; Grätzel, M.; Hagfeldt, A. Using a Two-Step Deposition Technique to Prepare Perovskite (CH$_3$NH$_3$PbI$_3$) for Thin Film Solar Cells Based on ZrO$_2$ and TiO$_2$ Mesostructures. *RSC Adv.* **2013**, *3*, 18762–18766. [CrossRef]

10. Liu, Z.; Cao, F.; Wang, M.; Wang, M.; Li, L. Observing Defect Passivation of the Grain Boundary with 2-Aminoterephthalic Acid for Efficient and Stable Perovskite Solar Cells. *Angew. Chem. Int. Ed.* **2020**, *59*, 4161–4167. [CrossRef]

11. Lee, D.G.; Kim, D.H.; Lee, J.M.; Kim, B.J.; Kim, J.Y.; Shin, S.S.; Jung, H.S. High Efficiency Perovskite Solar Cells Exceeding 22% via a Photo-Assisted Two-Step Sequential Deposition. *Adv. Funct. Mater.* **2021**, *31*, 2006718. [CrossRef]

12. Chen, Y.; Tan, S.; Li, N.; Huang, B.; Niu, X.; Li, L.; Sun, M.; Zhang, Y.; Zhang, X.; Zhu, C.; et al. Self-Elimination of Intrinsic Defects Improves the Low-Temperature Performance of Perovskite Photovoltaics. *Joule* **2020**, *4*, 1961–1976. [CrossRef]

13. Ahlawat, P.; Hinderhofer, A.; Alharbi, E.A.; Lu, H.; Ummadisingu, A.; Niu, H.; Invernizzi, M.; Zakeeruddin, S.M.; Dar, M.I.; Schreiber, F.; et al. A Combined Molecular Dynamics and Experimental Study Of two-Step Process Enabling Low-Temperature Formation of Phase-Pure α-FAPbI$_3$. *Sci. Adv.* **2021**, *7*, eabe3326. [CrossRef] [PubMed]

14. Burschka, J.; Pellet, N.; Moon, S.J.; Humphry-Baker, R.; Gao, P.; Nazeeruddin, M.K.; Grätzel, M. Sequential Deposition as a Route to High-Performance Perovskite-Sensitized Solar Cells. *Nature* **2013**, *499*, 316–319. [CrossRef]

15. Im, J.H.; Jang, I.H.; Pellet, N.; Grätzel, M.; Park, N.G. Growth of CH$_3$NH$_3$PbI$_3$ Cuboids with Controlled Size for High-Efficiency Perovskite Solar Cells. *Nat. Nanotechnol.* **2014**, *9*, 927–932. [CrossRef]

16. Jiang, Q.; Chu, Z.; Wang, P.; Yang, X.; Liu, H.; Wang, Y.; Yin, Z.; Wu, J.; Zhang, X.; You, J. Planar-Structure Perovskite Solar Cells with Efficiency beyond 21%. *Adv. Mater.* **2017**, *29*, 1703852. [CrossRef]

17. Qin, M.; Xue, H.; Zhang, H.; Hu, H.; Liu, K.; Li, Y.; Qin, Z.; Ma, J.; Zhu, H.; Yan, K.; et al. Precise Control of Perovskite Crystallization Kinetics via Sequential A-Site Doping. *Adv. Mater.* **2020**, *32*, 2004630. [CrossRef]

18. Xiong, Z.; Chen, X.; Zhang, B.; Odunmbaku, G.O.; Ou, Z.; Guo, B.; Yang, K.; Kan, Z.; Lu, S.; Chen, S.; et al. Simultaneous Interfacial Modification and Crystallization Control by Biguanide Hydrochloride for Stable Perovskite Solar Cells with PCE of 24.4%. *Adv. Mater.* **2022**, *34*, 2106118. [CrossRef]

19. Fu, Y.; Meng, F.; Rowley, M.B.; Thompson, B.J.; Shearer, M.J.; Ma, D.; Hamers, R.J.; Wright, J.C.; Jin, S. Solution Growth of Single Crystal Methylammonium Lead Halide Perovskite Nanostructures for Optoelectronic and Photovoltaic Applications. *J. Am. Chem. Soc.* **2015**, *137*, 5810–5818. [CrossRef] [PubMed]

20. Liu, T.; Hu, Q.; Wu, J.; Chen, K.; Zhao, L.; Liu, F.; Wang, C.; Lu, H.; Jia, S.; Russell, T.; et al. Mesoporous PbI$_2$ Scaffold for High-Performance Planar Heterojunction Perovskite Solar Cells. *Adv. Energy Mater.* **2016**, *6*, 1501890. [CrossRef]

21. Hsieh, T.Y.; Huang, C.K.; Su, T.-S.; Hong, C.Y.; Wei, T.C. Crystal Growth and Dissolution of Methylammonium Lead Iodide Perovskite in Sequential Deposition: Correlation between Morphology Evolution and Photovoltaic Performance. *ACS Appl. Mater. Interfaces* **2017**, *9*, 8623–8633. [CrossRef] [PubMed]

22. Zheng, E.; Wang, X.F.; Song, J.; Yan, L.; Tian, W.; Miyasaka, T. PbI2-Based Dipping-Controlled Material Conversion for Compact Layer Free Perovskite Solar Cells. *ACS Appl. Mater. Interfaces* **2015**, *7*, 18156–18162. [CrossRef] [PubMed]

23. Jiang, C.; Lim, S.L.; Goh, W.P.; Wei, F.X.; Zhang, J. Improvement of $CH_3NH_3PbI_3$ Formation for Efficient and Better Reproducible Mesoscopic Perovskite Solar Cells. *ACS Appl. Mater. Interfaces* **2015**, *7*, 24726–24732. [CrossRef]

24. Song, J.; Yang, Y.; Zhao, Y.L.; Che, M.; Zhu, L.; Gu, X.Q.; Qiang, Y.H. Morphology Modification of Perovskite Film by a Simple Post-Treatment Process in Perovskite Solar Cell. *Mater. Sci. Eng. B Solid-State Mater. Adv. Technol.* **2017**, *217*, 18–25. [CrossRef]

25. Li, S.; Ren, H.; Yan, Y. Boosting Efficiency of Planar Heterojunction Perovskite Solar Cells to 21.2% by a Facile Two-Step Deposition Strategy. *Appl. Surf. Sci.* **2019**, *484*, 1191–1197. [CrossRef]

26. Zhao, Y.; Li, Q.; Zhou, W.; Hou, Y.; Zhao, Y.; Fu, R.; Yu, D.; Liu, X.; Zhao, Q. Double-Side-Passivated Perovskite Solar Cells with Ultra-Low Potential Loss. *Sol. RRL* **2019**, *3*, 1800296. [CrossRef]

27. Hui, W.; Chao, L.; Lu, H.; Xia, F.; Wei, Q.; Su, Z.; Niu, T.; Tao, L.; Du, B.; Li, D.; et al. Stabilizing Black-Phase Formamidinium Perovskite Formation at Room Temperature and High Humidity. *Science* **2021**, *371*, 1359–1364. [CrossRef]

28. Yao, Y.; Zou, X.; Cheng, J.; Chen, D.; Chang, C.; Ling, T.; Ren, H. Impact of Delay Time before Annealing MAI-PbI_2-DMSO Intermediate Phase on Perovskite Film Quality and Photo-Physical Properties. *Crystals* **2019**, *9*, 151. [CrossRef]

29. Im, J.H.; Kim, H.S.; Park, N.G. Morphology-Photovoltaic Property Correlation in Perovskite Solar Cells: One-Step versus Two-Step Deposition of $CH_3NH_3PbI_3$. *APL Mater.* **2014**, *2*, 81510. [CrossRef]

30. Xiao, Z.; Bi, C.; Shao, Y.; Dong, Q.; Wang, Q.; Yuan, Y.; Wang, C.; Gao, Y.; Huang, J. Efficient, High Yield Perovskite Photovoltaic Devices Grown by Interdiffusion of Solution-Processed Precursor Stacking Layers. *Energy Environ. Sci.* **2014**, *7*, 2619–2623. [CrossRef]

31. Ahn, N.; Kang, S.M.; Lee, J.W.; Choi, M.; Park, N.G. Thermodynamic Regulation of $CH_3NH_3PbI_3$ Crystal Growth and Its Effect on Photovoltaic Performance of Perovskite Solar Cells. *J. Mater. Chem. A* **2015**, *3*, 19901–19906. [CrossRef]

32. Ko, H.; Sin, D.H.; Kim, M.; Cho, K. Predicting the Morphology of Perovskite Thin Films Produced by Sequential Deposition Method: A Crystal Growth Dynamics Study. *Chem. Mater.* **2017**, *29*, 1165–1174. [CrossRef]

33. Chauhan, M.; Zhong, Y.; Schötz, K.; Tripathi, B.; Köhler, A.; Huettner, S.; Panzer, F. Investigating Two-Step MAPbI_3 Thin Film Formation during Spin Coating by Simultaneous: In Situ Absorption and Photoluminescence Spectroscopy. *J. Mater. Chem. A* **2020**, *8*, 5086–5094. [CrossRef]

34. Borchert, J.; Milot, R.L.; Patel, J.B.; Davies, C.L.; Wright, A.D.; Martínez Maestro, L.; Snaith, H.J.; Herz, L.M.; Johnston, M.B. Large-Area, Highly Uniform Evaporated Formamidinium Lead Triiodide Thin Films for Solar Cells. *ACS Energy Lett.* **2017**, *2*, 2799–2804. [CrossRef]

35. Liu, M.; Johnston, M.B.; Snaith, H.J. Efficient Planar Heterojunction Perovskite Solar Cells by Vapour Deposition. *Nature* **2013**, *501*, 395–398. [CrossRef]

36. Luo, L.; Ku, Z.; Li, W.; Zheng, X.; Li, X.; Huang, F.; Peng, Y.; Ding, L.; Cheng, Y.B. 19.59% Efficiency from Rb0.04-Cs0.14FA0.86Pb(BryI1−y)3 Perovskite Solar Cells Made by Vapor–solid Reaction Technique. *Sci. Bull.* **2021**, *66*, 962–964. [CrossRef]

37. Peng, Y.; Jing, G.; Cui, T. A Hybrid Physical-Chemical Deposition Process at Ultra-Low Temperatures for High-Performance Perovskite Solar Cells. *J. Mater. Chem. A* **2015**, *3*, 12436–12442. [CrossRef]

38. Soltanpoor, W.; Dreessen, C.; Sahiner, M.C.; Susic, I.; Afshord, A.Z.; Chirvony, V.S.; Boix, P.P.; Gunbas, G.; Yerci, S.; Bolink, H.J. Hybrid Vapor-Solution Sequentially Deposited Mixed-Halide Perovskite Solar Cells. *ACS Appl. Energy Mater.* **2020**, *3*, 8257–8265. [CrossRef]

39. Chen, C.-W.; Kang, H.-W.; Hsiao, S.-Y.; Yang, P.-F.; Chiang, K.-M.; Lin, H.-W. Efficient and Uniform Planar-Type Perovskite Solar Cells by Simple Sequential Vacuum Deposition. *Adv. Mater.* **2014**, *26*, 6647–6652. [CrossRef]

40. Leyden, M.R.; Ono, L.K.; Raga, S.R.; Kato, Y.; Wang, S.; Qi, Y. High Performance Perovskite Solar Cells by Hybrid Chemical Vapor Deposition. *J. Mater. Chem. A* **2014**, *2*, 18742–18745. [CrossRef]

41. Qiu, L.; He, S.; Jiang, Y.; Qi, Y. Metal Halide Perovskite Solar Cells by Modified Chemical Vapor Deposition. *J. Mater. Chem. A* **2021**, *9*, 22759–22780. [CrossRef]

42. Qiu, L.; He, S.; Jiang, Y.; Son, D.Y.; Ono, L.K.; Liu, Z.; Kim, T.; Bouloumis, T.; Kazaoui, S.; Qi, Y. Hybrid Chemical Vapor Deposition Enables Scalable and Stable Cs-FA Mixed Cation Perovskite Solar Modules with a Designated Area of 91.8 cm^2 Approaching 10% Efficiency. *J. Mater. Chem. A* **2019**, *7*, 6920–6929. [CrossRef]

43. Shen, P.S.; Chen, J.S.; Chiang, Y.H.; Li, M.H.; Guo, T.F.; Chen, P. Low-Pressure Hybrid Chemical Vapor Growth for Efficient Perovskite Solar Cells and Large-Area Module. *Adv. Mater. Interfaces* **2016**, *3*, 1500849. [CrossRef]

44. Xiang, W.; Zhang, J.; Liu, S.; Albrecht, S.; Hagfeldt, A.; Wang, Z. Intermediate Phase Engineering of Halide Perovskites for Photovoltaics. *Joule* **2022**, *6*, 315–339. [CrossRef]

45. Xiang, Y.; Ma, Z.; Huang, Y.; Zhang, W.; Peng, C.; Li, H. Strategy for Crystallization Management of Perovskite: Incorporation of FAI in a PbI_2 Precursor for a Two-Step Spin-Coating Process. *ACS Appl. Energy Mater.* **2021**, *4*, 12091–12098. [CrossRef]

46. Tong, G.; Son, D.Y.; Ono, L.K.; Liu, Y.; Hu, Y.; Zhang, H.; Jamshaid, A.; Qiu, L.; Liu, Z.; Qi, Y. Scalable Fabrication of >90 cm^2 Perovskite Solar Modules with >1000 H Operational Stability Based on the Intermediate Phase Strategy. *Adv. Energy Mater.* **2021**, *11*, 2003712. [CrossRef]

47. Zuo, L.; Guo, H.; DeQuilettes, D.W.; Jariwala, S.; De Marco, N.; Dong, S.; DeBlock, R.; Ginger, D.S.; Dunn, B.; Wang, M.; et al. Polymer-Modified Halide Perovskite Films for Efficient and Stable Planar Heterojunction Solar Cells. *Sci. Adv.* **2017**, *3*, e1700106. [CrossRef] [PubMed]

48. Ge, C.; Lu, J.F.; Singh, M.; Ng, A.; Yu, W.; Lin, H.; Satapathi, S.; Hu, H. Mixed Dimensional Perovskites Heterostructure for Highly Efficient and Stable Perovskite Solar Cells. *Sol. RRL* **2021**, *6*, 2100879. [CrossRef]

49. Xiao, Y.; Yang, L.; Han, G.; Li, Y.; Li, M.; Li, H. Effects of Methylammonium Acetate on the Perovskite Film Quality for the Perovskite Solar Cell. *Org. Electron.* **2019**, *65*, 201–206. [CrossRef]

50. Yang, L.; Ma, X.; Shang, X.; Gao, D.; Wang, C.; Li, M.; Chen, C.; Zhang, B.; Xu, S.; Zheng, S.; et al. Zwitterionic Ionic Liquid Confer Defect Tolerance, High Conductivity, and Hydrophobicity toward Efficient Perovskite Solar Cells Exceeding 22% Efficiency. *Sol. RRL* **2021**, *5*, 2100352. [CrossRef]

51. Zhang, H.; Qin, M.; Chen, Z.; Yu, W.; Ren, Z.; Liu, K.; Huang, J.; Zhang, Y.; Liang, Q.; Chandran, H.T.; et al. Bottom-Up Quasi-Epitaxial Growth of Hybrid Perovskite from Solution Process—Achieving High-Efficiency Solar Cells via Template-Guided Crystallization. *Adv. Mater.* **2021**, *33*, 2100009. [CrossRef]

52. Gong, X.; Guan, L.; Pan, H.; Sun, Q.; Zhao, X.; Li, H.; Pan, H.; Shen, Y.; Shao, Y.; Sun, L.; et al. Highly Efficient Perovskite Solar Cells via Nickel Passivation. *Adv. Funct. Mater.* **2018**, *28*, 1804286. [CrossRef]

53. Su, L.; Xiao, Y.; Han, G.; Lu, L.; Li, H.; Zhu, M. Performance Enhancement of Perovskite Solar Cells Using Trimesic Acid Additive in the Two-Step Solution Method. *J. Power Sources* **2019**, *426*, 11–15. [CrossRef]

54. Abzieher, T.; Mathies, F.; Hetterich, M.; Welle, A.; Gerthsen, D.; Lemmer, U.; Paetzold, U.W.; Powalla, M. Additive-Assisted Crystallization Dynamics in Two-Step Fabrication of Perovskite Solar Cells. *Phys. Status Solidi Appl. Mater. Sci.* **2017**, *214*, 1700509. [CrossRef]

55. Li, N.; Zhu, Z.; Chueh, C.C.; Liu, H.; Peng, B.; Petrone, A.; Li, X.; Wang, L.; Jen, A.K.Y. Mixed Cation FAxPEA1–xPbI3 with Enhanced Phase and Ambient Stability toward High-Performance Perovskite Solar Cells. *Adv. Energy Mater.* **2017**, *7*, 1601307. [CrossRef]

56. Li, W.; Fan, J.; Li, J.; Mai, Y.; Wang, L. Controllable Grain Morphology of Perovskite Absorber Film by Molecular Self-Assembly toward Efficient Solar Cell Exceeding 17%. *J. Am. Chem. Soc.* **2015**, *137*, 10399–10405. [CrossRef]

57. Chen, P.; Zhang, Y.; Du, J.; Wang, Y.; Zhang, X.; Liu, Y. Global Control of $CH_3NH_3PbI_3$ Formation with Multifunctional Ionic Liquid for Perovskite Hybrid Photovoltaics. *J. Phys. Chem. C* **2018**, *122*, 10699–10705. [CrossRef]

58. Chen, Y.; Li, N.; Wang, L.; Li, L.; Xu, Z.; Jiao, H.; Liu, P.; Zhu, C.; Zai, H.; Sun, M.; et al. Impacts of Alkaline on the Defects Property and Crystallization Kinetics in Perovskite Solar Cells. *Nat. Commun.* **2019**, *10*, 1112. [CrossRef]

59. Cai, F.; Yan, Y.; Yao, J.; Wang, P.; Wang, H.; Gurney, R.S.; Liu, D.; Wang, T. Ionic Additive Engineering Toward High-Efficiency Perovskite Solar Cells with Reduced Grain Boundaries and Trap Density. *Adv. Funct. Mater.* **2018**, *28*, 1801985. [CrossRef]

60. Cao, J.; Wang, F.; Yu, H.; Zhou, Y.; Lu, H.; Zhao, N.; Wong, C.P. Porous PbI_2 Films for the Fabrication of Efficient, Stable Perovskite Solar Cells: Via Sequential Deposition. *J. Mater. Chem. A* **2016**, *4*, 10223–10230. [CrossRef]

61. Zhou, G.; Wu, J.; Zhao, Y.; Li, Y.; Shi, J.; Li, Y.; Wu, H.; Li, D.; Luo, Y.; Meng, Q. Application of Cesium on the Restriction of Precursor Crystallization for Highly Reproducible Perovskite Solar Cells Exceeding 20% Efficiency. *ACS Appl. Mater. Interfaces* **2018**, *10*, 9503–9513. [CrossRef] [PubMed]

62. Tai, Q.; You, P.; Sang, H.; Liu, Z.; Hu, C.; Chan, H.L.W.; Yan, F. Efficient and Stable Perovskite Solar Cells Prepared in Ambient Air Irrespective of the Humidity. *Nat. Commun.* **2016**, *7*, 11105. [CrossRef]

63. Yang, W.S.; Park, B.W.; Jung, E.H.; Jeon, N.J.; Kim, Y.C.; Lee, D.U.; Shin, S.S.; Seo, J.; Kim, E.K.; Noh, J.H.; et al. Iodide Management in Formamidinium-Lead-Halide-Based Perovskite Layers for Efficient Solar Cells. *Science* **2017**, *356*, 1376–1379. [CrossRef] [PubMed]

64. Wu, Y.; Islam, A.; Yang, X.; Qin, C.; Liu, J.; Zhang, K.; Peng, W.; Han, L. Retarding the Crystallization of PbI_2 for Highly Reproducible Planar-Structured Perovskite Solar Cells via Sequential Deposition. *Energy Environ. Sci.* **2014**, *7*, 2934–2938. [CrossRef]

65. Cao, X.; Zhi, L.; Li, Y.; Fang, F.; Cui, X.; Yao, Y.; Ci, L.; Ding, K.; Wei, J. Control of the Morphology of PbI_2 Films for Efficient Perovskite Solar Cells by Strong Lewis Base Additives. *J. Mater. Chem. C* **2017**, *5*, 7458–7464. [CrossRef]

66. Shahbazi, S.; Li, M.Y.; Fathi, A.; Diau, E.W.G. Realizing a Cosolvent System for Stable Tin-Based Perovskite Solar Cells Using a Two-Step Deposition Approach. *ACS Energy Lett.* **2020**, *5*, 2508–2511. [CrossRef]

67. Liu, X.; Wu, T.; Luo, X.; Wang, H.; Furue, M.; Bessho, T.; Zhang, Y.; Nakazaki, J.; Segawa, H.; Han, L. Lead-Free Perovskite Solar Cells with Over 10% Efficiency and Size 1 cm^2 Enabled by Solvent–Crystallization Regulation in a Two-Step Deposition Method. *ACS Energy Lett.* **2022**, *7*, 425–431. [CrossRef]

68. Han, Y.; Xie, H.; Lim, E.L.; Bi, D. Review of Two-Step Method for Lead Halide Perovskite Solar Cells. *Sol. RRL* **2022**, 2101007. [CrossRef]

69. Zhang, C.; Wang, Y.; Lin, X.; Wu, T.; Han, Q.; Zhang, Y.; Han, L. Effects of A Site Doping on the Crystallization of Perovskite Films. *J. Mater. Chem. A* **2021**, *9*, 1372–1394. [CrossRef]

70. Yu, B.B.; Chen, Z.; Zhu, Y.; Wang, Y.; Han, B.; Chen, G.; Zhang, X.; Du, Z.; He, Z. Heterogeneous 2D/3D Tin-Halides Perovskite Solar Cells with Certified Conversion Efficiency Breaking 14%. *Adv. Mater.* **2021**, *33*, 2102055. [CrossRef]